Role of Molecular Weight of Atactic Poly(vinyl alcohol) (PVA) in the Structure and Properties of PVA Nanofabric Prepared by Electrospinning

Joon Seok Lee,[1] Kyu Ha Choi,[1] Han Do Ghim,[1] Sam Soo Kim,[1] Du Hwan Chun,[1] Hak Yong Kim,[2] Won Seok Lyoo[1]

[1]School of Textiles, Yeungnam University, Kyongsan 712-749, Korea
[2]Depatment of Textile Engineering, Chonbuk National University, Chon-ju 561-756, Korea

ABSTRACT: Atactic poly(vinyl alcohols) (a-PVAs) having number-average degrees of polymerization [(P_n)s] of 1700 and 4000 were prepared by the solution polymerization of vinyl acetate, which was followed by the saponification of poly(vinyl acetate) to investigate the effects of molecular weights of a-PVA on the characteristics of electrospun a-PVA nanofabrics. A-PVA nanofabrics were prepared by electrospinning with controlling the process parameters including the electrical field, conductivity, tip-to-collector distance, and solution concentration. Through a series of char-

acterization experiments, we identified that the molecular weight of a-PVA had a marked influence on the structure and properties of nanofabrics produced. That is, the higher the molecular weight of PVA, the superior the physical properties of PVA nanofabric. © 2004 Wiley Periodicals, Inc. J Appl Polym Sci 93: 1638–1646, 2004

Key words: PVA; molecular weight; nanofabric; electrospinning; process parameter

INTRODUCTION

Poly(vinyl alcohol) (PVA), obtained by the saponification of poly(vinyl ester) or poly(vinyl ether), has been of interest because of its good properties and various usages. The excellent chemical resistance, physical properties, and biocompatibility of PVA resins have led to their broad practical applications such as fibers for clothes and industries, adhesives and binders, films, membranes, materials for drug delivery system, and cancer cell-killing embolic materials.[1–3] PVA fiber has high tensile and compressive strengths, tensile modulus, and abrasion resistance due to its highest crystalline lattice modulus. Molecular parameters, like molecular weight, degree of saponification, and syndiotacticity, can be controlled to maximize these physical properties of PVA.[4–14] Especially, molecular weight is a fundamental parameter affecting the physical properties of PVA.[7,13]

Nanomaterials of minute dimensions can be rationally designed to exhibit novel properties, phenomena, and processes.[15] There are many methods to prepare nanomaterials. Among them, electrospinning is a straightforward one that produces polymer nanofabrics. When the electrical force at the surface of a poly-

mer solution or polymer melt overcomes the surface tension, a charged jet is ejected. The jet extends in a straight line for a certain distance, and then bends and follows a looping and spiraling path. The electrical forces elongate of the jet thousands even millions of times, and the jet becomes very thin. Ultimately, the solvent evaporates, or the melt solidifies. The resulting very long, nanofiber collects on an electrically grounded metal sheet, a winder or some other object, often in the form of a nonwoven fabric. Generally, the electrospinning process makes fabrics with diameters of one or two orders of magnitude smaller than those of conventional textile fabrics. The small diameter provides a large surface area-to-mass ratio, ranging from 10 to 1000 m^2/g. The equipment required for electrospinning is simple, and only a small amount of polymer sample is needed to produce nanofabrics.

Electrospinning involves many scientific fields, including polymer science, applied physics, fluid mechanics, electrical, mechanical, chemical, and material engineering, rheology, and so on. Therefore, many parameters, including the electric field, solution viscosity, resistivity, surface tension, charge carried by the jet, and relaxation time can affect the process. A comprehensive mathematical model of this process was developed by Reneker et al.[16] The electrospinning process has three stages: (1) jet initiation and the extension of the jet along a straight line; (2) the growth of a bending instability and the further elongation of the

TABLE I
Solution Polymerization Conditions of VAc

Type of initiator	ADMVN
Type of solvent	DMSO
Initiator concentration	0.0001 mol/mol of VAc
	0.00005 mol/mol of VAc
Monomer concentration	4 mol/mol of solvent
	9 mol/mol of solvent
Temperature	40°C

jet, which allows the jet to become very long and thin while it follows a looping and spiraling path; (3) solidification of the jet into nanofabrics.

In a typical experiment, a pendent droplet of polymer solution was supported by surface tension at the tip of the spinneret. When the electrical potential difference between the spinneret and the grounded collector was increased, the motion of ions through the liquid charged the surface of the liquid. The electrical forces at the surface overcame the forces associated with surface tension. An electrically charged liquid jet emerged from a conical protrusion that formed on the surface of the pendant droplet. It carried away the ions that were attracted to the surface when the potential was applied, and the charge density on the jet and the flow rate of the jet were increased with an increase in the potential.

In this study, we prepared two different atactic PVA (a-PVA) nanofabrics having number-average degrees of polymerization [(P_n)s] of 1700 (medium molecular weight) and 4000 (high molecular weight [HMW]), respectively, through electrospinning with varying process parameters, such as electrical field, tip-to-collector distance (TCD), and solution concentration. Optimum electrospinning conditions were deduced through a series of characterization methods including scanning electron microscopy (SEM), differential scanning calorimetry (DSC), thermogravimetric analyzer (TGA), wide-angle X-ray diffractometer (WAXD), and Instron.

EXPERIMENTAL

Solution polymerization of VAc

VAc was placed in a three-necked round-bottom flask and flushed with dry nitrogen. The dimethyl sulfoxide (DMSO) was added into a flask to dissolve the solid monomer and flushed with nitrogen for 3 h to eliminate oxygen. At the predetermined polymerization temperature, 2,2'-azobis(2,4-dimethyl-valeronitrile) (ADMVN) was added to solution. At the completion of polymerization, the unreacted monomer was distilled out. PVAc was reprecipitated several times from *n*-hexane and then dried under vacuum at 50°C for 24 h. Conversion was calculated by measuring the weight of the polymer. Conversions were averages of

five determinations. The detailed polymerization conditions are given in Table I.

Saponification of PVAc

To a solution of 2 g of PVAc in 100 mL of methanol, 2.5 mL of 40% NaOH aqueous solution was added, and the mixture was stirred for 5 h at room temperature to yield a-PVA. The a-PVA produced was filtered and washed well with methanol.

Acetylation of PVA

A mixture of 1 g of PVA, 2 mL of pyridine, 20 mL of acetic anhydride, and 20 mL of acetic acid was stirred in a three-necked flask at 100°C for 24 h under an atmosphere of nitrogen. Then the mixture was poured into cold water to precipitate PVAc. The PVAc thus produced was filtered and purified by repeating the reprecipitation from methanol and water.

Electrospinning of a-PVA

PVA was dissolved in water at 90°C for 2 h and maintained for 30 min to ensure homogenization. Concentration of PVA aqueous solution was varied from 5 to 15 wt %. Figure 1 showed the schematic representation of electrospinning apparatus. PVA solution in a capillary tube, which was fixed above a grounded tubular layer, formed a droplet due to the weight. By applied voltage, the droplet was instantly disintegrated into fibers that were drawn to the tubular layer. Applied voltage was ranged from 5 to 30 kV. TCD was varied from 5 to 15 cm. The critical voltage, crossdirection width, and throughput were checked during the electrospinning process.

Characterization

The P_n of PVA was determined by the viscosity measurement of the fully reacetylated specimen in ben-
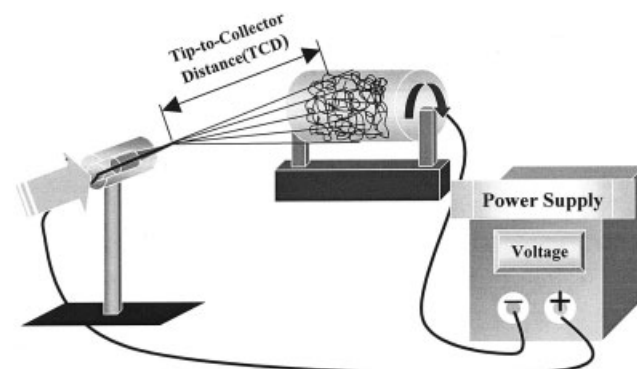

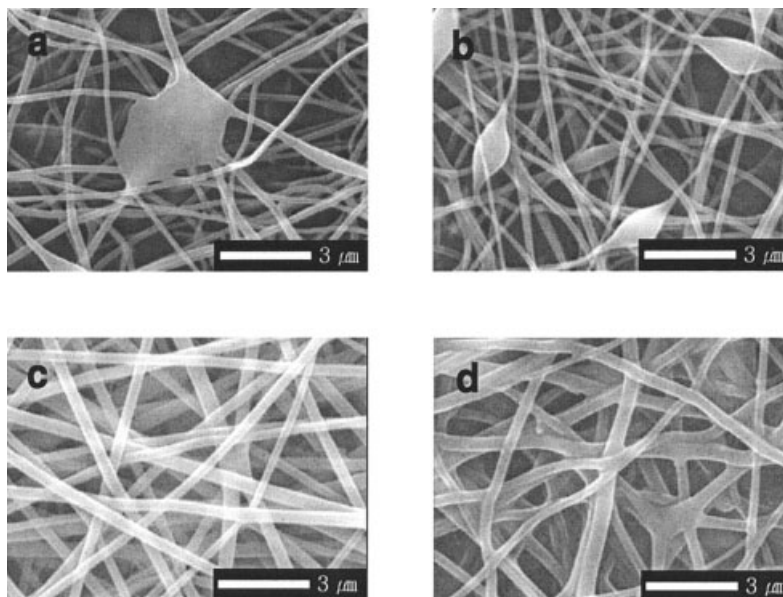**Figure 1** Schematic representation of the electrospinning process.

Figure 2 SEM photographs of an a-PVA nanofiber having a P_n of 1700 electrospun at an applied voltage and TCD of 20 kV and 10 cm, respectively, with solution concentrations: (a) 6 wt %; (b) 8 wt %; (c) 10 wt %; (d) 12 wt %.

zene solution with an Ubbelohde viscometer. Measured intrinsic viscosity, $[\eta]$, was converted into P_n by eq. (1).[17,18]

$$[\eta] = 8.91 \times 10^{-3}[P_n]^{0.62} \text{ (in benzene at 30°C)} \quad (1)$$

The fiber morphology and fiber diameter of the electrospun PVA fiber were determined using SEM (HITACHI, S-4100). A small section of the fiber mat was placed on the SEM sample holder and sputter coated with gold (HITACHI, E-1030). Accelerating voltage of 15 kV was employed to take the photographs.

WAXD diffractograms were obtained with nickel-filtered CuKα radiation (26 kV, 6 mA) and diffraction patterns were obtained with a Laue camera (RIGAKU, D/MXP-2200H). The measurement of the crystallinity was carried out at room temperature with a Philips diffractometer, with a Geiger counter, connected to a computer. The diffraction scans were collected at $2\theta = 3$–50°.

The crystal melting temperature (T_m) of the PVA fabric was measured by using DSC (Perkins-Elmer, DSC) with a sample weight of 10 mg and at a heating rate of 10°C/min. The thermogravimetric analysis of PVA fabric was conducted by using TGA (Perkins-Elmer, TGA-7) with a sample weight of 5 mg and at a heating rate of 10°C/min.

The mechanical properties of PVA fabric were determined with an Instron 4301 (Automated Materials Testing System 1.23 series IX). The extension rate was 100 mm/min at 20°C. Specimens were prepared in the crossdirection and machine direction (2 cm wide, 5 cm long, and 40–70 μm thick).

RESULTS AND DISCUSSION

To select the suitable electrospinning conditions producing the thinner and the more uniform PVA nanofiber, we performed a series of experiments with varying electrospinning parameters, including concentration of PVA solution, applied voltage, TCD, and molecular weight of PVA. Microscopic and fiber diameter distribution studies for evaluating the optimum electrospinning conditions of various polymer systems were conducted by several researchers. Demir et al.[19] reported the effects of these parameters on the electrospinning behavior of elastomeric polyurethane copolymer using microscopic methods, including optical microscope, SEM, and atomic force microscope. Effects of electrospinning parameters on the morphological change, especially the beaded structure of the nanofiber, were conducted by Fong et al.[20] Morphological studies were also performed by Deitzel et al.,[21] Sukigara et al.,[22] Pawlowski et al.,[23] and Ohgo et al.[24] They used SEM as a main characterization method.

Figure 2 showed the SEM photographs of a-PVA fabrics (P_n of 1700) prepared from the electrospinning at various concentrations. Applied voltage and TCD were fixed to 20 kV and 10 cm, respectively. At a low solution concentration, the split ability of a droplet was high enough to exhibit the aggregated bulk as shown in Figure 2(a). This aggregated bulk was changed to a bead and finely arrayed nanofiber with increasing solution concentrations [Fig. 2(b) and (c)]. The split ability was reduced with increasing solution concentration because of the increased viscosity and the surface tension. Figure 2(d) showed the bonded nanofiber electrospun at a high concentration over
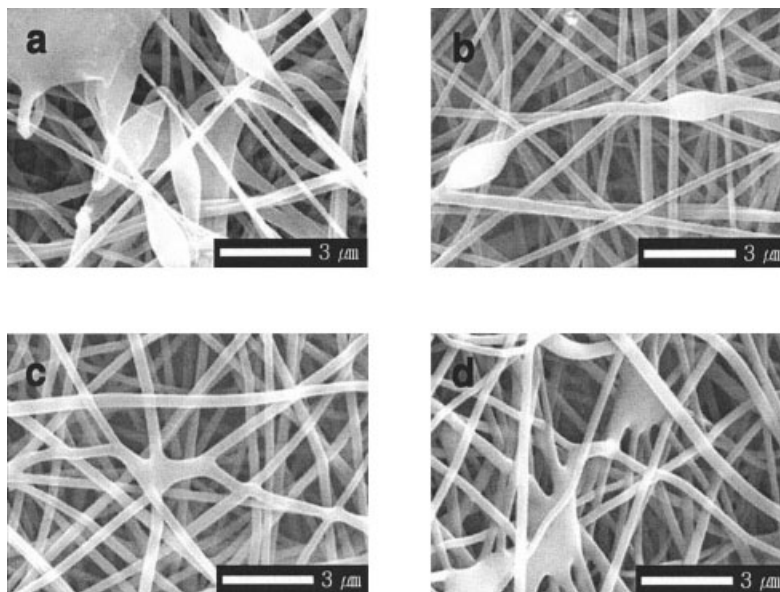
Figure 3 SEM photographs of an a-PVA nanofiber having a P_n of 4000 electrospun at an applied voltage and TCD of 20 kV and 10 cm, respectively, with solution concentrations: (a) 5 wt %; (b) 6 wt %; (c) 7 wt %; (d) 8 wt %.

optimum. As the viscosity of the solution was increased, the beads were larger, the average distance between beads was longer, the fiber diameter was larger, and the shape of the beads changed from spherical to spindle-like. As the excess charge density increased, the beads became smaller and more spindle-like, while the diameter of fibers became smaller. These tendencies were also observed in the cases of HMW PVA nanofabrics having a P_n of 4000, as shown in Figure 3. From these results, it can be deduced that a-PVAs having (P_n)s of 1700 and 4000 have the opti-

mum concentration at 10 and 7 wt %, respectively, at a presented applied voltage and TCD. Lower optimum polymer concentration was obtained at a higher molecular weight.

The electrospray process could be sustained in a variety of modes characterized by the shape of the surface from which the liquid jet originated. These modes occurred at different voltages, and have significant effects on droplet size distribution and current transport.[27] It has been verified experimentally that the shape of the initiating drop changes with spinning
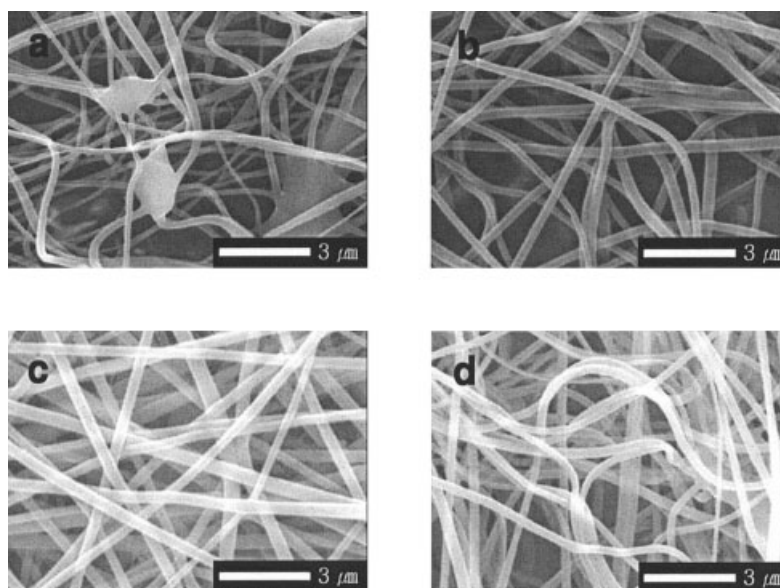

Figure 4 SEM photographs of an a-PVA nanofabric having a P_n of 1700 electrospun at a TCD and solution concentration of 10 cm and 10 wt %, respectively, with applied voltages: (a) 10 kV; (b) 15 kV; (c) 20 kV; (d) 25 kV.
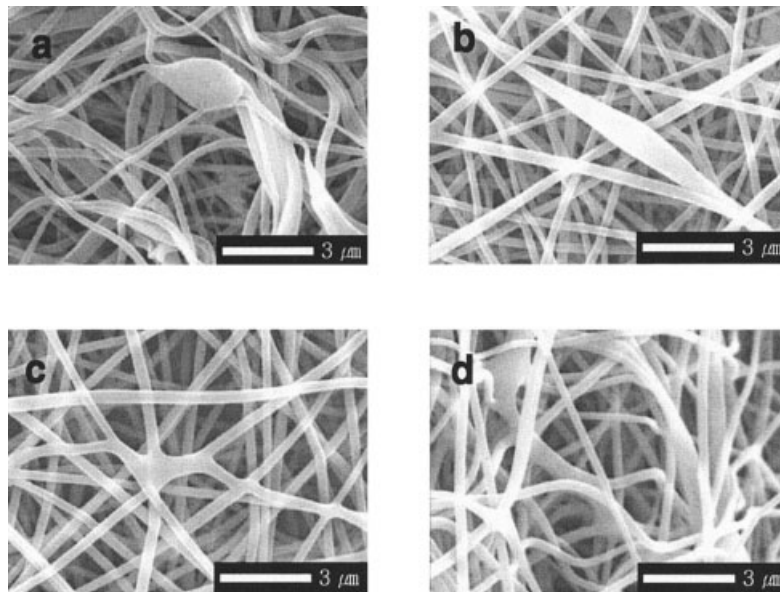
Figure 5 SEM photographs of an a-PVA nanofabric having a P_n of 4000 electrospun at a TCD and solution concentration of 10 cm and 7 wt %, respectively, with applied voltages: (a) 10 kV; (b) 15 kV; (c) 20 kV; (d) 25 kV.

conditions (voltage, viscosity, feed rate).[28] It was known that the electrostatic force was gradually increased with increasing the voltage. The split ability of the droplet was reinforced due to the increasing the electrostatic force. Increasing the voltage causes the rate at which the solution was removed from the capillary tip to exceed the rate of delivery of the solution to the tip needed to maintain the conical shape of the surface. Higher net charge density of droplet guarantees the low surface tension. Therefore, high net charge density is also important as well as high concentration to prevent the formation of beads. Figure 4 showed the effects of applied voltage on the morphological changes of electrospun a-PVA having a P_n of 1700 at a concentration and TCD of 10 wt % and 10 cm, respectively. With increasing the applied voltage, PVA nanofibers become finer. At an applied voltage of 25 kV, however, the formation of a loop was observed due to the excessively increased voltage to break the ideal balloon. The net charge density of the droplet was thought not to be affected by the molecular weight of the PVA because HMW a-PVA having a P_n of 4000 showed a similar relationship, as shown in Figure 5. From these results, it was supposed that the optimum voltage applied during the electrospinning of a-PVA was thought to be 20 kV. The effects of the applied voltage on the average diameters of a-PVAs electrospun at various concentrations were shown in Figure 6. The fiber became thinner with increasing the applied voltage. Loop structure, however, was developed at 25 kV due to the severely of the reduced surface tension.

Figures 7 and 8 showed the SEM photographs of PVA nanofabrics having (P_n)s of 1700 and 4000, re-

spectively, electrospun at various (TCD)s. At a TCD of 5 cm, two specimens showed bead formation; this was attributed to the incompletely shaped balloon during the electrospinning. As shown in Figure 9, the lowest average fiber diameter was obtained at 7 cm for both cases. However, it was impossible to obtain an evenly constituted nanoweb at this condition because of the severe fluctuation in diameters. As the TCD was increased, the average diameters of the nanofiber were increased because of the reduction in the effective
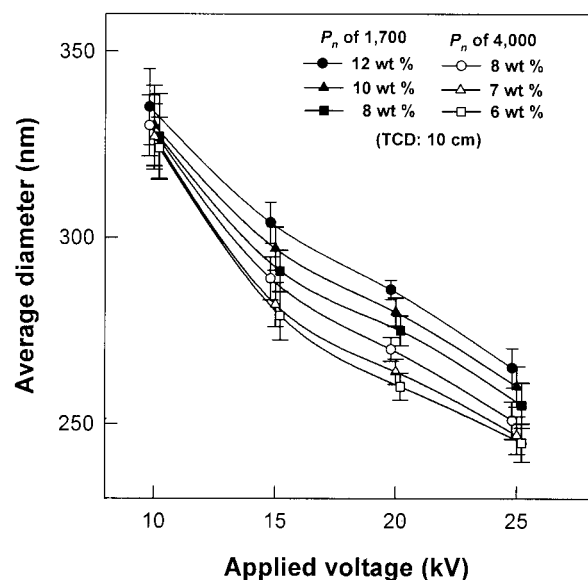

Figure 6 Average diameters of a-PVA nanofibers as functions of an applied voltage and solution concentration: TCD: 10 cm.
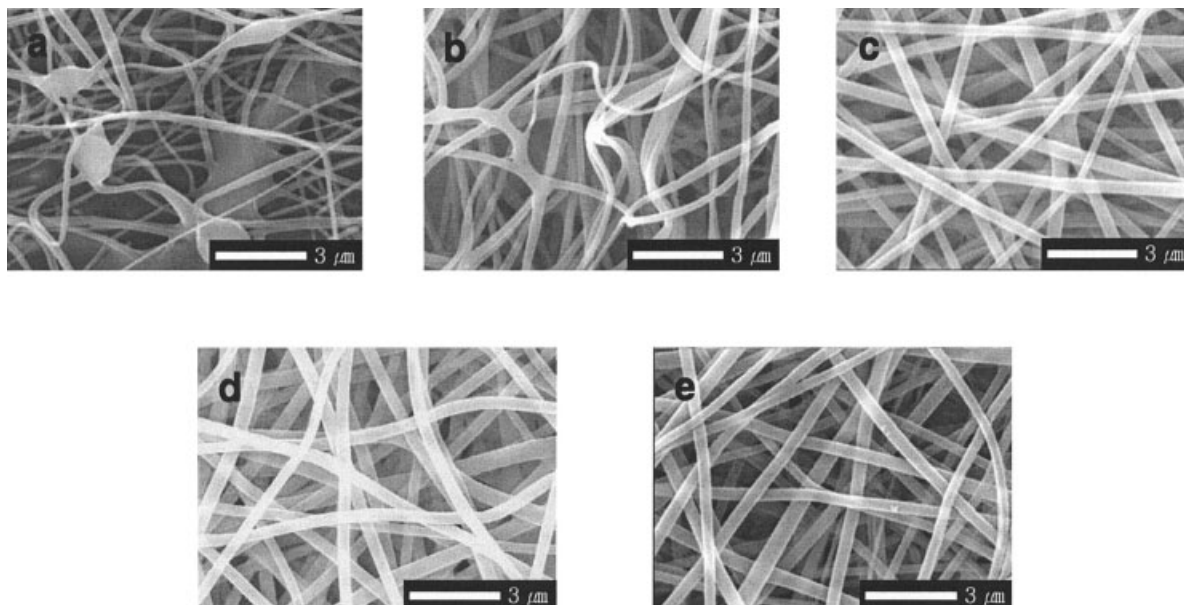
Figure 7 SEM photographs of an a-PVA nanofabric having a P_n of 1700 electrospun at a solution concentration and applied voltage of 10 wt % and 20 kV, respectively, with (TCD)s: (a) 5 cm; (b) 7 cm; (c) 10 cm; (d) 13 cm; (e) 15 cm.

voltage. From these results, it was possible to establish the optimum conditions for electrospinning of PVAs of this study.

Figure 10(a) and (b) showed the fiber diameter distributions of a-PVAs having (P_n)s of 1700 and 4000, respectively, which were electrospun at optimum conditions for each. PVA specimens of this study showed the average values of diameter at about 270–280 nm with narrow distributions.

WAXD patterns of a-PVA nanofabrics prepared at optimum conditions were presented in Figure 11. Compared with those of the PVA having a P_n of 4000, the reflections of the fabric pattern of PVA having a P_n of 1700 were relatively broad and obscure. Meanwhile, the WAXD pattern of the PVA having a P_n of 4000 also contained numerous higher order reflections that could not be seen in the pattern of the low molecular weight PVA. As shown in
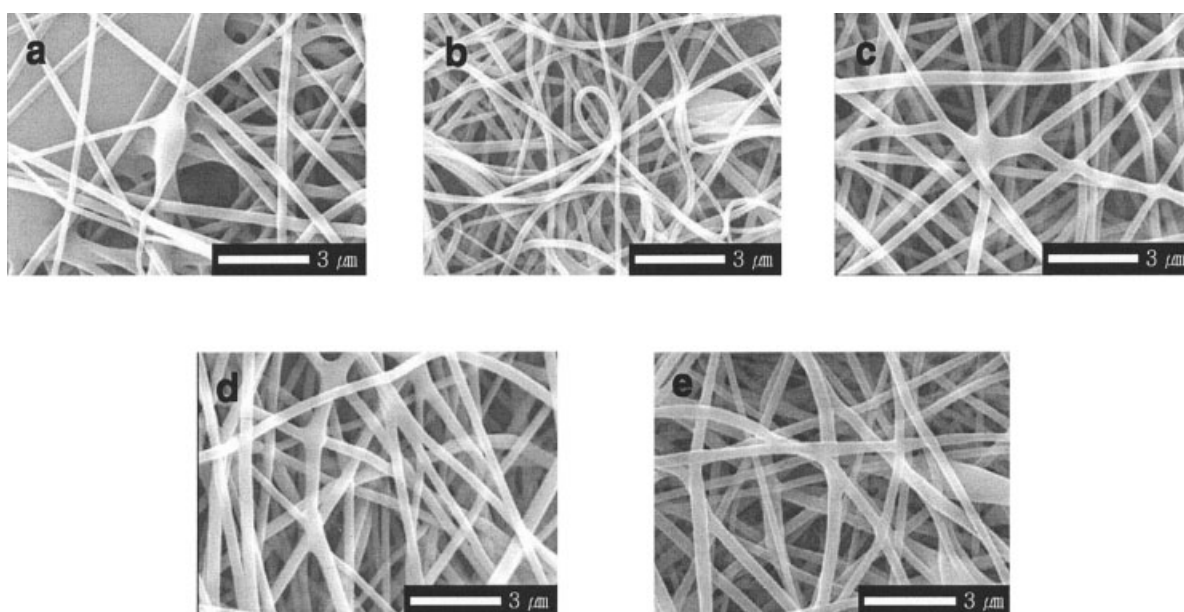

Figure 8 SEM photographs of an a-PVA nanofabric having a P_n of 4000 electrospun at a solution concentration and an applied voltage of 7 wt % and 20 kV, respectively, with (TCD)s: (a) 5 cm; (b) 7 cm; (c) 10 cm; (d) 13 cm; (e) 15 cm.
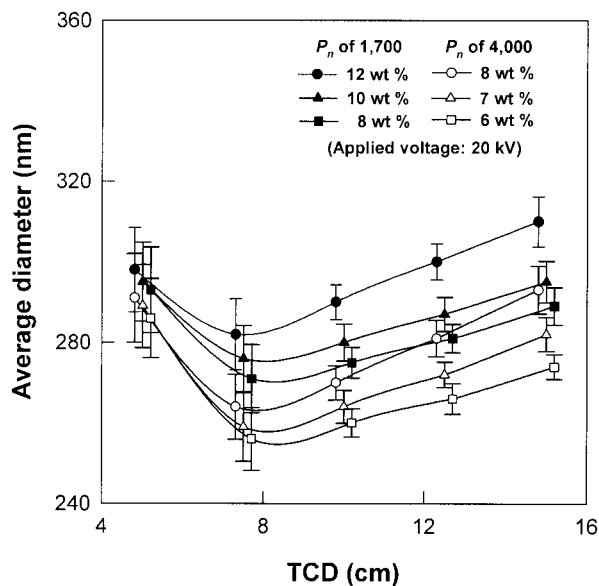
Figure 9 Average diameters of a-PVA nanofibers as functions of TCD and solution concentration: applied voltage: 20 kV.

Figure 11, two peaks around $2\theta = 10°$ and $2\theta = 20°$ appeared, corresponding to the (001) and (101) plains of PVA crystalline, respectively. PVA nanofabric having a P_n of 4000 showed higher and sharper intensities for these two peaks. This was ascribed to the higher crystallinity and orientation of the PVA having a P_n of 4000 due to the higher chain length and higher linearity.

Shao et al.[25] and Ding et al.[26] used thermal analysis by DSC as well as morphological study to evaluate the effects of processing variables of electrospinning. Ding et al.[26] analyzed the crosslinking properties of the PVA nanofiber using SEM and DSC. Figure 12 showed DSC thermograms of two PVA nanofabrics derived from a-PVAs having (P_n)s of 1700 and 4000 by electrospinning at optimum conditions. From the DSC thermogram of PVA having a P_n of 1700 one large peak was observed at about 224.7°C, respectively. The peak at 224.7°C was assigned T_m of PVA having a P_n of 1700, which was shifted to 232.7°C for PVA having a P_n of 4000 due to the higher molecular weight and resulting effective crystalline structure.

Generally, a-PVA, when it is pyrolyzed in the absence of oxygen, undergoes dehydration and de-
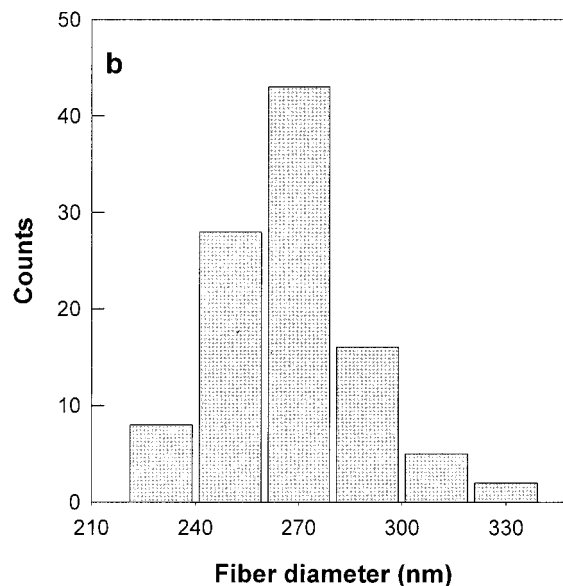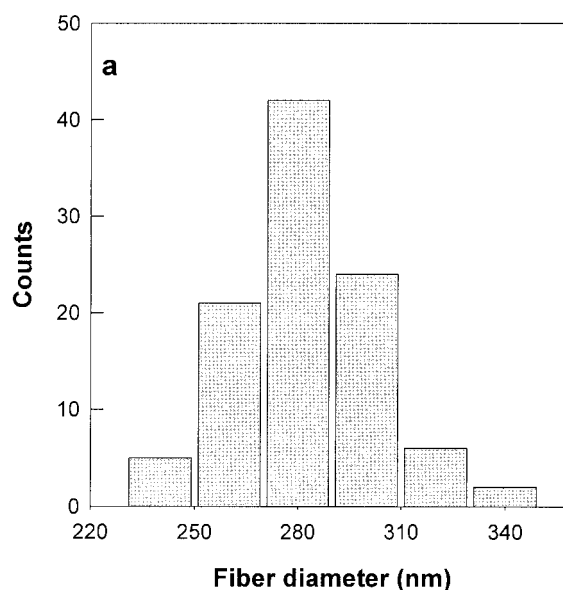

Figure 10 Frequency distribution of diameters of a-PVA nanofibers prepared at optimum conditions: P_n of a-PVA: (a) 1700; (b) 4000.

polymerization at over 200 and 400°C, respectively. Its thermal stability is dependent on the synthesizing method. Tsuchiya and Sumi[27] showed that water was eliminated from the PVA chain at 245°C, resulting in formation of a conjugated polyene as follows:
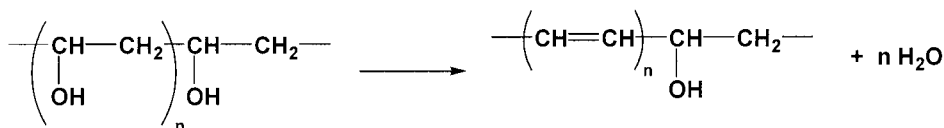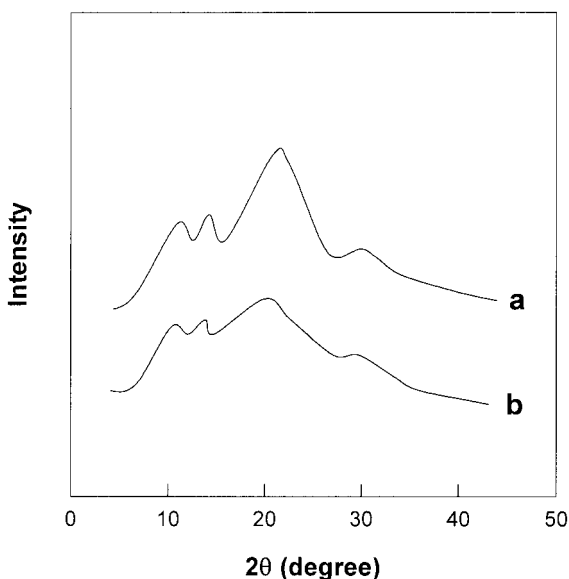
Figure 11 WAXD patterns of a-PVA nanofabrics: P_n of a-PVA: (a) 1,700; (b) 4000.
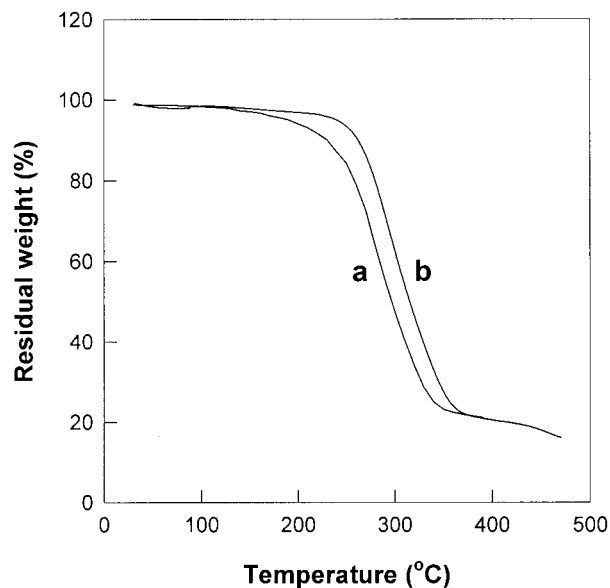

Figure 13 TGA thermograms of a-PVA nanofabrics: P_n of a-PVA: (a) 1700; (b) 4000.

The higher thermal stability of the high molecular weight PVA might be attributed to its higher chain compactness due to the tight intermolecular hydrogen bonding, as presented in Figure 13.

Figure 14 showed the stress–strain relationship of PVA nanofabrics prepared at optimum conditions for each. PVA nanofabric having a P_n of 1700 showed the tensile modulus and yield strength of 1.0 GPa and 16 MPa, respectively, which were increased to 1.2 GPa and 18 MPa for a PVA of 4000. However, two specimens showed similar elongation at yielding, at about

0.02%. It is concluded that higher molecular weight is required for obtaining PVA nanofabric with high performance.

CONCLUSIONS

Optimum electrospinning conditions for a-PVAs having (P_n)s of 1700 and 4000, respectively, were determined through morphological investigation. At these conditions, nanofabrics having average diameters of 300 and 240 nm for a-PVAs having (P_n)s of 1700 and
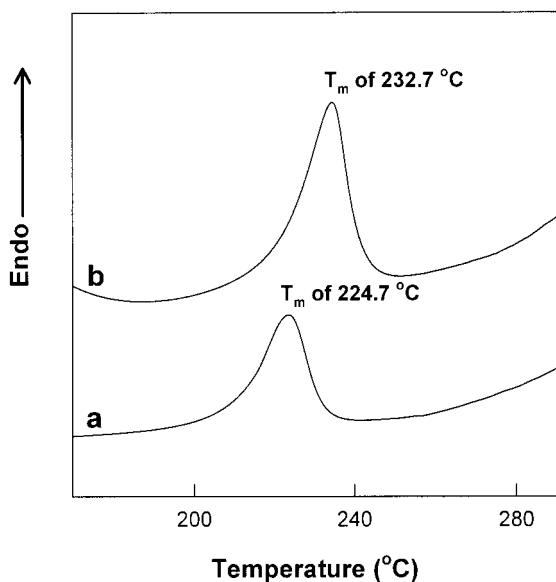

Figure 12 DSC thermograms of a-PVA nanofabrics: P_n of a-PVA: (a) 1700; (b) 4000.
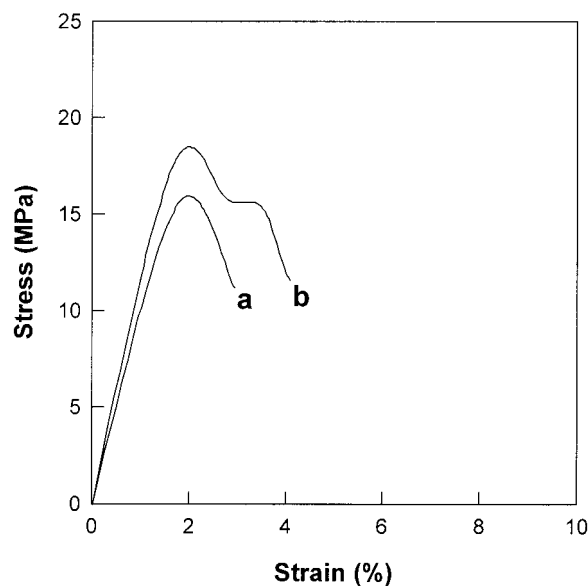

Figure 14 Stress–strain curves of a-PVA nanofabrics: P_n of a-PVA: (a) 1700; (b) 4000.

4000, respectively, were successfully produced. The average diameter of a-PVA nanofiber was slightly decreased with an increase in the electrical potential and with decreases in TCD and solution concentration. A-PVA of a higher P_n could be prepared at a lower solution concentration and higher applied voltage. An A-PVA nanofabric of higher molecular weight showed superior crystalline property, thermal stability, and mechanical property to a lower one. It is concluded that higher molecular weight is required for obtaining a PVA nanofabric with a high performance. In the near future, we will report on the electrospinning of stereo-regular PVA.

References

1. Mark, H. F.; Bikales, N. N.; Overberger, C. G.; Nenges, G. Encyclopedia of Polymer Science and Engineering; Wiley: Chichester, England, 1989; p 62.
2. Masuda, M. In Polyvinyl Alcohol—Developments; Finch, C. A., Ed.; John Wiley & Sons: New York, 1991; pp 403, 711.
3. Sakurada, I. In Polyvinyl Alcohol Fibers; Lewin, M., Ed.; Marcel Dekker: New York, 1985; pp 3, 361.
4. Lyoo, W. S.; Ha, W. S. Polymer 1996, 37, 3121.
5. Cho, J. D.; Lyoo, W. S.; Chvalun, S. N.; Blackwell, J. Macromolecules 1999, 32, 6236.
6. Choi, J. H.; Lyoo, W. S.; Ko, S. W. Macromol Chem Phys 1999, 200, 1421.
7. Lyoo, W. S.; Han, S. S.; Choi, J. H.; Cho, Y. W.; Ha, W. S. J Kor Fiber Soc 1995, 32, 1023.
8. Lyoo, W. S.; Ha, W. S. Polymer 1999, 40, 497.
9. Lyoo, W. S.; Chvalun, S. N.; Ghim, H. D.; Kim, J. P.; Blackwell, J. Macromolecules 2001, 34, 2615.
10. Lyoo, W. S.; Kim, J. H.; Choi, J. H.; Kim, B. C.; Blackwell, J. Macromolecules 2001, 34, 3982.
11. Lyoo, W. S.; Kim J. H.; Koo, K.; Lee, J. S.; Kim, S. S.; Yoon, W. S.; Ji, B. C.; Kwon, I. C.; Lee, C. J. J Polym Sci Part B Polym Phys 2001, 39, 1263.
12. Lyoo, W. S.; Yeum, J. H.; Chim, H. D.; Ji, B. C.; Yoon, W. S.; Kim, J. P. Ha, J Kor Fiber Soc 2000, 37, 487.
13. Lyoo, W. S.; Yeum, J. H.; Ghim, H. D.; Ji, B. C.; Yoon, N. S.; Ha, J. B.; Lee, J. J Appl Polym Sci 2003, 90, 227.
14. Lyoo, W. S.; Blackwell, J.; Ghim, H. D. Macromolecules 1998, 31, 4253.
15. Borisenko, V. E.; Filonor, A. B., Physics Chemistry and Application of Nanostructures; World Scientific: Singapore, 1999; p 324.
16. Reneker, D. H.; Yarin, A. L.; Fong, H.; Koomhongse, S. J Appl Phys 2000, 87, 4531.
17. Lyoo, W. S.; Ha, W. S. J Kor Fiber Soc 1996, 33, 156.
18. Lyoo, W. S.; Kwark, Y. J.; Ha, W. S. J Kor Fiber Soc 1996, 33, 321.
19. Demir, M. M.; Yilgor, I.; Yilgor, E.; Erman, B. Polymer 2002, 43, 3303.
20. Fong, H.; Chun, I.; Reneker, D. H. Polymer 1999, 40, 4585.
21. Deitzel, J. M.; Kleinmeyer, J.; Harris, D.; Beck Tan, N. C. Polymer 2001, 42, 261.
22. Sukigara, S.; Gandhi, M.; Ayutsede, J.; Micklus, M.; Ko, F. Polymer 2003, 44, 5721.
23. Pawlowski, K. J.; Belvin, H. L.; Raney, D. L.; Su, J.; Harrison, J. S.; Siochi, E. J. Polymer 2003, 44, 1309.
24. Ohgo, K.; Zhao, C.; Kobayashi, M.; Asakura, T. Polymer 2003, 44, 841.
25. Shao, C.; Kim, H. Y.; Gong, J.; Ding, B.; Lee, D. R.; Park, S. J. Mater Lett 2003, 57, 1579.
26. Ding, B.; Kim, H. Y.; Lee, S. C.; Lee, D. R.; Choi, K. J. Fiber Polym 2002, 3, 73.
27. Deitzel, J. M.; Kleinmeyer, J. D.; Hirvonen, J. K.; Beek Tan, N. C. Polymer 2001, 42, 8163.
28. Gibson, P.; Gibson, H. S.; Rivin, D. Colloids Surfaces A Physicochem Eng Aspects 2001, 187, 469.
29. Tsuchiya, Y.; Sumi, K. J Polym Sci Part A Polym Chem 1969, 7, 3151.